Biomedicine & Pharmacotherapy 181 (2024) 117712

Contents lists available at ScienceDirect

Biomedicine & Pharmacotherapy

journal homepage: www.elsevier.com/locate/biopha

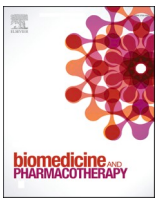

Pacritinib prevents inflammation-driven myelofibrosis-like phenotype in a *miR-146a*$^{-/-}$ murine model

Ernesto José Cuenca-Zamora [a,b,c,d,1], Constantino Martínez [a,1], María Luz Morales [a,d], Pedro Jesús Guijarro-Carrillo [a], María José López-Poveda [e], Carlos Alcolea-Guardiola [e], Natalia Vidal-Garrido [a], María Luisa Lozano [a,b,c], Rocío Gonzalez-Conejero [a,c], Raúl Teruel-Montoya [a,b,c,d,*,2], Francisca Ferrer-Marín [a,b,c,d,*,2]

[a] Hematology Department, Hospital Universitario Morales-Meseguer, Centro Regional de Hemodonación, IMIB-Pascual Parrilla, Murcia, Spain
[b] CIBERER-ISCIII CB15/00055 (U765), Spain
[c] Universidad de Murcia, Murcia, Spain
[d] Universidad Católica San Antonio (UCAM), Murcia, Spain
[e] Servicio de Anatomía Patológica. H.U. Morales Meseguer, Murcia, Spain

ARTICLE INFO

Keywords:
Myeloproliferative neoplasms
Myelofibrosis
Inflammation
miR-146a
Pacritinib
IRAK1

ABSTRACT

Chronic proinflammatory signaling is a characteristic trait in myeloproliferative neoplasms (MPN), particularly myelofibrosis (MF). Aberrant inflammatory signaling, particularly from NF-κB pathway, exacerbates the progression of MPN. Previously, we identified a critical role of miR-146a, a negative regulator of the TLR/NF-κB axis, in MF development. MPN patients carrying the miR-146a rs2431697-TT genotype, associated with lower miR-146a expression levels, have a higher risk of progression to overt-MF from chronic-phase disease. Using *miR-146a*$^{-/-}$ (KO) mice, a MF-like model lacking MPN driver mutations, we here investigate whether pacritinib, a dual JAK/NF-κB pathways inhibitor (via JAK2/IRAK1, respectively), prevents the age-associated myelofibrotic phenotype of these mice. Young *miR-146a*$^{-/-}$ mice were treated either with or without pacritinib, for 3 or 6 months. Notably, pacritinib prevented the splenomegaly, reticulin fibrosis and osteosclerosis observed in untreated KO mice. Pacritinib also avoided the myeloproliferation, loss of splenic architecture, and extramedullary hematopoiesis observed in age-matched untreated KO mice. Pharmacological targeting of IRAK1/JAK2 attenuated the pro-inflammatory environment, preventing the increase of inflammatory cytokines, particularly CXCL1 and TNF-α, without inducing cytopenias but rather the opposite. Compared to age-matched untreated KO mice, treated mice showed higher platelet counts irrespective of treatment duration, and higher erythrocyte counts with the longer treatment. Additionally, pacritinib preventive treatment reduced *COL1A1* production in an *in vitro* model mimicking *JAK2*-driven fibrosis. These findings highlight that dual inhibition of JAK2/IRAK1 with pacritinib, by delaying or attenuating the myelofibrotic progression, could be a potential modifier of the natural course of MPN.

1. Introduction

Philadelphia-negative myeloproliferative neoplasms (MPN) are a group of clonal hematopoietic stem and progenitor cell hemopathies (HSPC) comprising polycythemia vera (PV), essential thrombocythemia (ET), and primary myelofibrosis (MF) [1,2]. Both PV and ET can

Abbreviations: BM, Bone marrow; ET, Essential thrombocytopenia; HSPC, Hematopoietic stem and progenitor cell hemopathies; MF, Myelofibrosis; MK, Megakaryocytes; MPN, Myeloproliferative neoplasm; PB, Peripheral blood; PV, Polycythemia vera; SD, Standard deviation; SEM, Standard error of the mean; SMF, Secondary myelofibrosis; WT, Wild-type.

* Corresponding authors at: Hematology Department, Hospital Universitario Morales-Meseguer, Centro Regional de Hemodonación, IMIB-Pascual Parrilla, Murcia, Spain

E-mail addresses: rtm1@um.es, raul.teruel@carm.es (R. Teruel-Montoya), fferrer@ucam.edu, fferrer@um.es (F. Ferrer-Marín).

[1] These authors shared first authorship.
[2] These authors shared senior authorship.

https://doi.org/10.1016/j.biopha.2024.117712
Received 12 August 2024; Received in revised form 22 November 2024; Accepted 25 November 2024
Available online 26 November 2024

progress to MF, referred to as secondary MF (sMF) [1–3], a more advanced stage with a worse prognosis [4,5]. The classical MPN share clinical features and a common molecular basis: abnormal constitutive activation of the JAK/STAT pathway through the acquisition of somatic mutations in driver genes (*JAK2*, *CALR*, *MPL*), although ~10 % of MPN patients lack the classical "driver mutations" [1,2,6,7]. In general, therefore, these mutations are the causative events that can singularly trigger the onset of MPN [1,2,8]. However, expansion and dominance of the mutated HSPC clone occurs in a minority of cases, suggesting that additional factors, following the acquisition of driver mutations, influence this process [8].

A growing body of evidence has shown that inflammation is one of the factors favoring the conversion of clonal hematopoiesis to MPN [8–11], as well as the progression of MPN to advanced stages such as MF or acute leukemia [12–17]. Dysregulation of the inflammatory cascade is a key characteristic of MPN, particularly in MF [18], accounting for most of the symptoms, and contribute to bone marrow (BM) fibrosis [11, 14,19], the latter leading to extramedullary hematopoiesis [20]. Notably, although the clinical benefits of JAK2 inhibition in monotherapy largely reflect anti-inflammatory effects, the current JAK2 inhibitors are not disease-modifying agents.

The NF-κB pathway is a key player in inflammation-induced carcinogenesis [21]. In addition, the JAK/STAT pathway, while primarily involved in hematopoiesis through JAK2 mediation, is also involved in inflammation through JAK1, although this distinction is not mutually exclusive [22]. Moreover, the NF-κB and JAK/STAT pathways are interrelated [21]. On the one hand, within the IRAK1/NF-κB axis, IRAK1 can directly phosphorylate STAT3 and induce its nuclear translocation independently of the Janus kinases [23,24]. On the other hand, the JAK/STAT pathway can be activated by the cytokine IL-6 from the NF-κB pathway [25]. Ultimately, the NF-κB and JAK/STAT pathways work together to drive progression to MF [13,26].

One of the post-transcriptional mechanisms of NF-κB pathway regulation is mediated by miR-146a, which prevents the translation of *IRAK1* and *TRAF6*, thereby turning off the pathway signaling by negative feedback [27]. De-repression of these genes in *miR-146a*$^{-/-}$ knockout mice results in myeloproliferation, splenomegaly, cytopenias, extramedullary hematopoiesis, and BM fibrosis with age, a MF-like phenotype [28–30]. We have previously shown that this phenotype is mediated by a gradual increase of STAT3 signaling in the myeloid population [31], indicating a low inflammatory profile with aging. Notably, in murine models of MF [32], deletion of STAT3 exclusively on the malignant clone did not normalize the excess of proinflammatory cytokines; and inhibition of both cell populations (malignant and non-malignant) is necessary to achieve a therapeutic effect *in vivo* [10, 12,33]. Because inflammation is driven by both malignant and non-malignant clones [12,13,15], the *miR-146a*$^{-/-}$ murine model, which depicts constitutive inflammatory pathway activation, is proving highly valuable model for examining the role of chronic inflammation, particularly the IRAK1/NF-κB axis, in the progression of MPN without interference from driver mutations.

Furthermore, in PV and ET patients, we have previously shown that the *MIR146A* rs2431697-TT genotype, which is associated with lower miR-146a levels, is an independent covariate for early progression to sMF [31]. Consistent with the genotype, these patients had higher plasma levels of inflammatory cytokines, such as IL-1β. Our results were further confirmed in an external, independent cohort of MPN patients [34]. Despite the increasingly comprehensive understanding of the mechanisms underlying MPN progression, current PV and ET treatments are exclusively focused on reducing the risk of vascular events using cytoreductive and antiplatelet agents for patients considered at high thrombotic risk and observation/antiplatelet agents for those at low risk.

Considering that MPN is a chronic hematological disorder characterized by a prolonged latency state and that inflammation precedes the onset of fibrosis [35], the question arises whether the current therapeutical approach should be reconsidered to include earlier intervention [9] especially in those patients at higher risk of progression to evolved MF (*e.g.* patients harboring the *MIR146A* rs2431697-TT genotype or prefibrotic MF).

In this scenario, using *miR-146a*$^{-/-}$ mice without MPN driver mutations, we investigate whether simultaneous inhibition of the JAK2 and IRAK1 pathways with the dual inhibitor pacritinib [36,37], can prevent or delay the appearance of the MF-like phenotype with age.

2. Materials and methods

2.1. Drug and murine model

B6.Cg-*Mir146*$^{tm1.1Bal}$/J mice (*miR-146a*$^{-/-}$ (KO), #016239, Jackson Laboratory) were back-crossed to a C57BL/6 J (wild-type, WT) background for at least 8 generations. WT littermates from the inbred population were used as controls for phenotype features. Mice of 3 months were used for the study. They were housed in individually ventilated cages (3–5 mice/cage) at the local animal facility (CEIB, Universidad de Murcia) with food and water available *ad libitum* throughout the study. While WT mice (n=20) were fed their routine diet (#D17022801, Research Diets), KO mice were fed their routine diet (n=17) or supplemented with pacritinib (250 mg/kg/day; n=20) (#D20121806, Research Diets), for 3 or 6 months (short- or long-term respectively). This final dose of pacritinib was calculated based on the food consumption of these mice over the provided diet containing 3 g/kg pacritinib. Both diets were kindly provided by CTI BioPharma Corp, a Sobi company. The experimental design is shown in Fig. S1. At endpoint, mice were anesthetized by isoflurane inhalation, and peripheral blood (PB) was collected via the retro-orbital sinus using heparinized capillary tubes (#749311, Brand). Cell counts of PB samples were analyzed using the ADVIA 120 Hematology System (Siemens Healthineers). Finally, mice were sacrificed by cervical dislocation, and spleens and femurs were collected for further processing. Furthermore, to evaluate the baseline model, the spleen and BM of the femurs and tibias of 3-month-old WT (n=12) and KO (n=12) mice were examined macroscopically. Experiments involving animals were conducted following national and international guidelines for animal care. This study was approved by the Ethical Committee on Animal Experimentation (CEEA) of the University of Murcia and CARM (reference A13200603).

2.2. Plasma cytokine determination

Mouse plasma was obtained after centrifugation of PB at 2000 g for 15 minutes and stored at −80°C until further analysis. Quantification of plasma cytokines was then performed using a custom Luminex assay (#MHSTCMAG-70K, Merck) including IL-6, CXCL1 and TNF-α, and a IL-1β high sensitivity ELISA (#HSLB00D, R&D).

2.3. Histology preparation

Spleens were measured, weighed, washed with DMEM 1x (#11965092, ThermoFisher), and divided into two parts: 1/3 for histology and 2/3 for protein extraction before disaggregation with ACK lysis buffer (#A1049201, ThermoFisher). Sections for histology were fixed in 4 % paraformaldehyde (#211511, PanReac) and counterstained with hematoxylin-eosin solution. Femurs were washed 1x in PBS, fixed in 4 % PFA, decalcified in 0.5 M EDTA buffer pH=7.8 (#409975000, ThermoFisher), embedded in paraffin, stained for reticulin detection (#5279399001, Roche), and counterstained with hematoxylin-eosin solution. Both spleen and femur BM sections were scanned at 40x in a slide scanner (Pannoramic MIDI II, 3DHISTECH) and photographed (Objective: 110x/0.95, Achroplan; Camera: pco.edge 4.2MP bi sCMOS, PCO; Software: Pannoramic Scanner 3.0.2.127553 RTM, 3DHISTECH). Images (.mrxs files) were visualized using SlideViewer 2.5 software (3DHISTECH).

2.4. Histological analysis

In the spleen, SlideViewer software was used to get the preserved lymphoid nodules areas and total spleen area in order to calculate the concentration (as nodules per square millimeter) and percentage of white pulp, both indicative of myeloproliferation. Additional histological analyses were performed blindly by at least 2 of the authors. In the spleen, as a sign of splenic extramedullary hematopoiesis, the number of megakaryocytes (MKs) was measured in at least 5 fields 40x. In addition, other 2 key features of advanced-stage MPN were evaluated, using human sample criteria: i) cytological dysplasia of splenic MKs [38]. Cytological dysplasia was graded as absence, mild/moderate-1, and moderate-2/severe when 0 %, 1–50 %, or >50 % of MKs were dysplastic, respectively. Dysplastic MKs were defined as those that were abnormally small (micro-MKs), with changes in nuclear size or lobulation (hypo- or hyperlobulated forms), hyperchromatic nuclei, or with an increased nuclear:cytoplasmic ratio (Fig. S2); and ii) the presence of MK clusters [39], defined as architectural dysplasia of MKs, graded as absence, mild (rare clusters of <5 MKs), moderate (several clusters of 5–10 MKs or any cluster of 50 MKs), or severe (multiple small clusters or diffuse areas of MKs).

As previously defined in BM from humans, we recorded: i) cellularity [40], as a percentage of cells in the marrow space; ii) reticulin fibrosis [41], as absence (not observed), mild/moderate (fine or dense reticulin fibers with few or some intersections), or severe (with extensive intersections); iii) osteosclerosis [42], as absence (not observed), mild (focal budding, hooks, spikes, or trabecular apposition), or moderate/severe (diffuse new bone formation with thickening of trabeculae, occasionally with focal or extensive interconnected network of new bone with complete effacement of marrow); and iv) MK cytological dysplasia, as stated above.

2.5. Immunoblotting

Immunoblotting of total disaggregated splenocytes lysates was performed as *previously described* [43], with minor modifications indicated in the corresponding figure legend.

2.6. Statistics

Continuous variables are presented as mean±SD (standard deviation) or mean±SEM (standard error of the mean), as appropriate. Outliers were removed using the ROUT method (Q=0.1 % or Q=0.5, as indicated). The Shapiro-Wilk test was used to test for normal distribution. Two-tailed Student's *t*-test or Mann-Whitney U test was used for comparisons between two groups, as appropriate. Discrete variables were expressed as frequencies and percentages, and comparisons between groups were made using the chi-squared (χ^2) test. All comparisons were made between untreated WT and untreated KO mice (*), and between treated and untreated KO mice (#) for each treatment time. All statistical analyses were performed with GraphPad Prism 9.4 software. P values are indicated as */#: p≤0.05, **/##: p≤0.01, ***/###: p≤0.001, ****/####: p≤0.0001. Additional information of *in vitro* experiments can be found in Supplementary Material.

3. Results

3.1. Pacritinib increased platelet counts and did not worsen anemia after long-term treatment

Consistent with their phenotype, untreated KO mice exhibited cytopenias with aging. Thus, whereas WT mice (represented in green) showed hematimetric parameters stable in peripheral blood, untreated KO mice (shown in red) displayed erythrocyte counts, hemoglobin and hematocrit significantly decreased with aging (9-month-old *vs*. 6-month-old) (Fig. S3A). Platelet counts in 6-month-old untreated KO mice are about half that of matched-age WT mice but remained stable with aging (Fig. S3B). Additionally, spleen from WT mice developed an increase in mass, but not in length from 3-month-old to older 6- and 9-month-old mice, in line with the corresponding growth and aging, however, according to the development of MF phenotype, untreated KO showed an exacerbated increase in both parameters (Fig. S3C). Specifically, compared to WT mice at the same age, untreated KO mice showed decreased erythrocyte count, which resulted in anemia and a substantial reduction in hematocrit particularly in older mice (9-month-old KO mice) (Fig. 1 A). Thrombocytopenia in these mice was accompanied by a decline in plateletcrit in 6-month-old mice ($p<0.0001$), and an increase in mean platelet volume at both ages (Fig. 1B). Regarding leukocytes, only 6-month-old untreated KO mice had lower leukocyte counts compared to their age-matched WT mice, and in all subpopulations tested (Fig. S4).

Compared to their untreated age-matched KO counterparts, whereas pacritinib-treated mice (shown in blue) for 3 months (short-term) showed a significant decrease in erythrocyte, hemoglobin, and hematocrit levels, in the long-term (after 6 months of treatment), pacritinib increased these 3 parameters, becoming statistically significant for erythrocyte count and hematocrit (Fig. 1 A). Although not significant, our results showed that all treated mice for 6 months had higher mean hemoglobin levels than untreated mice (10.77 g/dL *vs.* 10.10 g/dL, respectively) (Fig. 1 A). In contrast to the erythrocyte count, short-term pacritinib treatment maintained platelet counts, platelecrit and mean platelet volume at levels similar to those of WT mice of the same age, *i.e.* prevented the thrombocytopenia seen in untreated KO, whereas long-term treatment significantly doubled the platelet count and plateletcrit (Fig. 1B). On the other hand, pacritinib did not affect total leukocyte counts at either treatment time point, although significantly decreased lymphocyte counts at short-term and increased neutrophil, monocyte and eosinophil levels at both time times (Fig. S4).

3.2. Aging-induced increase in proinflammatory cytokines was avoided by JAK2/IRAK1 inhibition

Next, we evaluated the effect of dual JAK2/IRAK1 inhibition with pacritinib on the increase in plasma proinflammatory cytokines described in this model [29,30]. As expected, untreated KO mice showed a trend towards higher levels of CXCL1, TNF-α, IL-1β, and IL-6 compared to their age-matched WT mice, with statistically significant differences in 6-month-old mice for CXCL1 ($p<0.05$) and IL-1β ($p<0.001$), and close to significance in IL-1β also in 6-month-old mice ($p=0.0676$) (Fig. 2 A). Pacritinib treatment attenuated the increase in proinflammatory cytokines levels. The differences were statistically significant for CXCL1 ($p<0.05$) and TNF-α ($p<0.05$) after 3 and 6 months of pacritinib treatment, respectively (Fig. 2 A). Expression levels of *Cxcl1*, *Tnf*, *Il1b* and *Il6* were also evaluated in spleen (Fig. 2B) and bone marrow (Fig. 2 C). Whereas *Cxcl1* and *Tnf* expression levels in untreated WT and KO mice, and pacritinib treated KO mice were concordant between plasma and bone marrow, *Il1b* levels showed the same expression profile in the three biological compartments examined. However, *Il6* profile levels were similar between spleen and bone marrow, but different to the behavior observed in plasma. Overall, these data demonstrate that long-term pacritinib treatment was able to maintain or reduce the levels of all the pro-inflammatory cytokines measured in plasma, spleen and bone marrow.

3.3. Dual JAK2/IRAK1 inhibition prevented, in vivo, splenomegaly and extramedullary hematopoiesis

Consistent with the literature [44], 3-month-old KO mice (before initiation of treatment) did not show the MF-like phenotype. KO mice showed no differences regarding splenomegaly (spleen length and mass), microscopic spleen appearance nor molecular levels of representative proteins of the JAK/STAT (pSTAT3/STAT3) and NF-κB

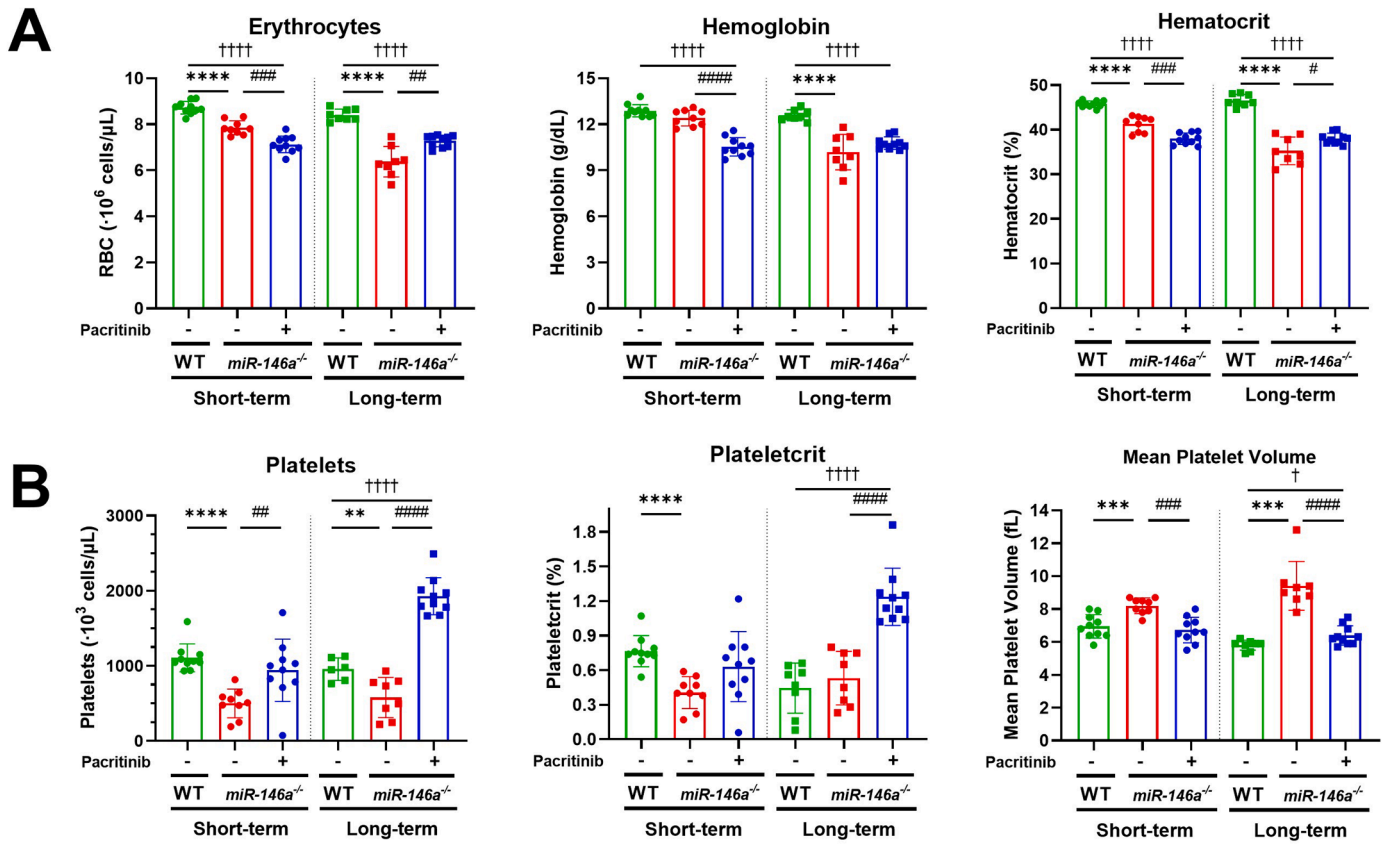

Fig. 1. Erythrocyte and platelet cytopenias, and CXCL1 and TNF-α increase were prevented in pacritinib-treated KO mice. (A) Erythrocyte, hemoglobin, hematocrit; (B) platelet, plateletcrit, mean platelet volume; and (C) plasma levels of CXCL1, TNF-α, IL-1β and IL-6 in WT and KO mice at endpoint. Outliers were removed using the ROUT method (Q=0.5 %). Graphs represent mean±SEM. Short-term: 6-month-old mice, after 3 months of diet with or without pacritinib. Long-term: 9-month-old mice, after 6 months of diet with or without pacritinib. Comparison between untreated WT and treated KO mice was included (†). */#/†: p≤0.05, **/##: p≤0.01, ***/###: p≤0.001, ****/####/††††: p≤0.0001 (n=8–10/group). RBC: Red blood cells.

(IRAK1, p65) signaling pathways (Fig. S5A-C). In addition, BM macroscopic and microscopic appearance was similar between both groups (Fig. S5D-E). As described, KO mice developed splenomegaly with aging (Fig. 3 A). Histologically, they showed myeloproliferation (Fig. 3B), as a sign of distortion of the spleen architecture with a lower density of lymphoid nodules (Fig. 3 C), and decreased white pulp (Fig. 3D), compared to their WT controls at the same age. Treatment with pacritinib for 3 or 6 months prevented the splenomegaly observed in untreated KO mice (Fig. 3 A). Regarding spleen architecture, short-term showed slight recovery (Fig. 3B), while long-term treatment with pacritinib significantly increased both, the concentration of lymphoid nodules (Fig. 3 C) as well as the percentage of white pulp (Fig. 3D), improving the visual distinction between red and white pulps.

As a sign of extramedullary hematopoiesis, untreated KO mice showed an increased number of MKs in the spleen (Fig. 4 A, 4B), which were dysplastic (Fig. 4 C, Fig. S2) and grouped in clusters (Fig. 4D), being the differences more pronounced in the 9-month-old KO-mice compared with their age-matched WT. Pacritinib treatment also prevented splenic extramedullary hematopoietic proliferation. Indeed, the number and architectural and morphological characteristics of MKs in treated KO mice were similar to those observed in age-matched WT mice (Fig. 4A-D).

To evaluate, *in vivo*, the effects of pacritinib treatment at the molecular level, NF-κB and JAK/STAT signaling was assessed in splenocyte lysates. Since untreated-KO mice develop statistically significant cellular [43] and histopathologic changes, with aging (Fig. 3B-D, Table S1), total spleen lysates between treated- and untreated-KO mice could not be compared. However, as pacritinib treatment preserved the architecture of the spleen, similarly to that observed in the age-matched WT mice (Table S1), the effects of pacritinib at a molecular level were evaluated between these groups. Our finding showed that, in *miR-146a*$^{-/-}$ mice, whereas pacritinib significantly inhibited the NF-κB signaling (IRAK1) both at short- and long-term, pTyr-STAT3/STAT3 levels were maintained to those observed for WT mice and slightly reduced after long-term treatment but without reaching statistical significance. Thus, we observed a slightly decrease in pTyr-STAT3/STAT3 levels after long-term treatment (Fig. 4E), while the effects on NF-κB signaling occurred earlier, after 3 months of treatment (for IRAK1, $p<0.01$) and were maintained after long-term treatment ($p<0.001$ and $p<0.0001$ for IRAK1 and p65, respectively) (Fig. 4E, Fig. S7).

3.4. *The myelofibrotic phenotype and osteosclerosis were notably prevented with the JAK2/IRAK1 inhibitor*

Consistent with the MF-like phenotype, the femurs of untreated KO mice showed a whitish coloration (Fig. 5 A), associated with a clear and significant increase in reticulin fibrosis and osteosclerosis at the microscopic level, along with increased cellularity, the presence of dysplastic MKs and higher expression of *Tgfb1* ($p<0.01$) (Fig. 5B-G, Fig. S2). To investigate whether JAK2/IRAK1 inhibition by pacritinib could also prevent or delay the onset of BM fibrosis, we performed macroscopic, microscopic histological studies and molecular analysis of the femurs of treated KO mice. Our results showed that pacritinib treatment for 3 or 6 months was able to prevent the myelofibrotic phenotype in KO mice, as pacritinib-treated KO mice showed a reddish coloration of the BM (Fig. 5 A) at both times points, consistent with the absence of reticulin fibrosis (Fig. 5B, C) and osteosclerosis (Fig. 5B, D), lower global cellularity (Fig. 5B, E), fewer dysplastic MKs (Figs. 5B, F,

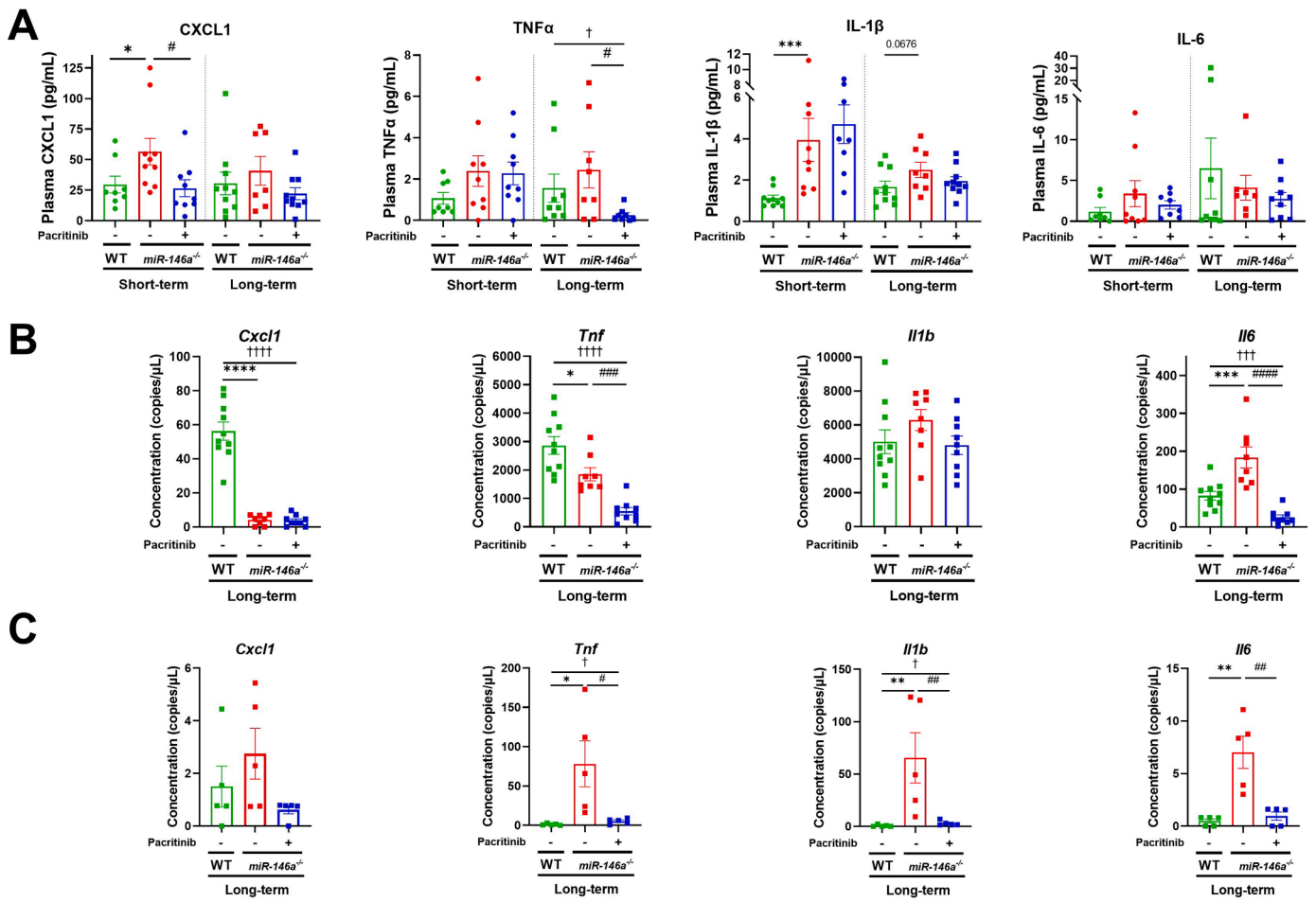

Fig. 2. Levels of pro-inflammatory cytokines in WT and KO mice at endpoint. (A) Plasma levels of CXCL1, TNF-α, IL-1β and IL-6 in untreated WT and KO mice, and short- and long- term pacritinib treated mice. (B) Expression levels of *Cxcl1*, *Tnf*, *Il1b* and *Il6* in spleen and (C) bone marrow from untreated WT and KO mice, and long-term pacritinib treated mice. Outliers were removed using the ROUT method (Q=0.1 %). Graphs represent mean±SEM. Short-term: 6-month-old mice, after 3 months of diet with or without pacritinib. Long-term: 9-month-old mice, after 6 months of diet with or without pacritinib. Comparison between untreated WT and treated KO mice was included (†). */#/†: p≤0.05, **/##: p<0.01, ***/###/†††: p≤0.001, ****/††††: p≤0.0001 (n=5–10/group).

Fig. S2) and lower expression of *Tgfb1* (Fig. 5 G) than untreated age-matched KO mice.

Taken together, our findings show that in an aberrant proinflammatory signaling environment, dual JAK2/IRAK1 inhibition with pacritinib prevented the myelofibrotic progression observed in untreated KO mice, maintaining a phenotype more similar to that observed in WT mice than in untreated KO mice (Table S1).

3.5. JAK2/IRAK1 inhibition reduced collagen expression, in vitro, in a JAK2V617F clonal hematopoiesis background

Finally, to further investigate whether dual JAK2/IRAK1 inhibition with pacritinib could prevent or delay collagen production in the BM microenvironment of MPN with driver mutations, we performed a coculture of collagen-producing BM-derived mesenchymal stromal cells (HS-27A) with *JAK2*V617F mutant cells (SET-2), as we previously described [43]. Notably, in a clonal MPN hematopoietic background using TGF-β as an inducer of collagen expression, prior treatment with pacritinib significantly decreased *COL1A1* expression in HS-27A cells ($p<0.05$) (Fig. S6).

4. Discussion

In this study, we hypothesized that the control of the inflammatory component associated with myeloproliferative disease might retard or avoid its progression. For this, we investigated whether dual JAK2/IRAK1 inhibitor pacritinib treatment in young *miR-146a*$^{-/-}$ mice could prevent the complete development of the myelofibrotic phenotype. The *miR-146a*$^{-/-}$ mouse was the chosen model since it develops a MF-like phenotype with age (cytopenias, elevated pro-inflammatory state, splenomegaly, extramedullary hematopoiesis, BM fibrosis, osteosclerosis and altered STAT signaling), like human MF [5], particularly triple-negative MF [6,16], as it lacks MPN driver mutations, but with activation of STAT3 signaling [31]. Other reported MPN murine models harboring canonical driver mutations show a similar phenotype than *miR-146a*$^{-/-}$ mouse model with slightly differences regarding disease latency [32]. These mice are phenotypically normal at birth [28], and no pathological phenotype has been reported until 8–10 weeks [44]. Importantly, our results confirmed our hypothesis, as the features of *miR-146a*$^{-/-}$ mice were more attenuated in treated than in untreated age-matched mice. Therefore, based on our findings, early treatment in subjects with high risk of progression to MF may be beneficial. Our findings are consistent with previous studies showing that early intervention with ruxolitinib in MF is associated with better treatment response (including fewer cytopenias) [45]. Thus, while short-term pacritinib treatment (3 months) appears to slightly decrease hemoglobin levels and hematocrit in young KO mice, a contrasting effect is observed after long-term treatment. These findings are consistent with recent clinical observations in patients with MF suggesting that although pacritinib can decrease hemoglobin levels [46], has a beneficial effect on

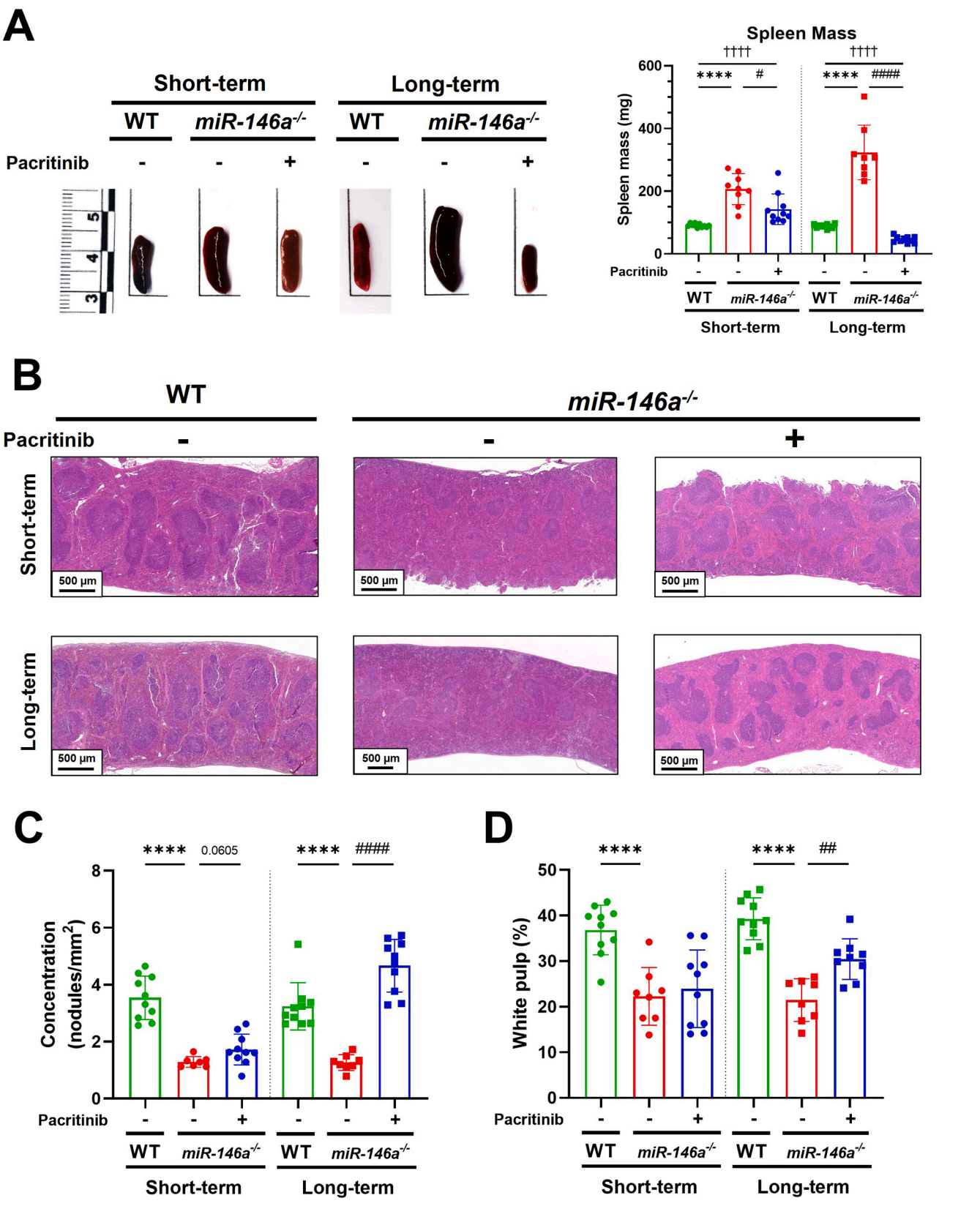

Fig. 3. Pacritinib treatment inhibited the development of splenomegaly and myeloproliferation in murine spleen. Macroscopic analysis: (A) Photographs of representative spleens from each group (mass around the mean of the corresponding group) and spleen mass at endpoint. Outliers were removed using the ROUT method (Q=0.1 %). Graph represents mean±SD. Comparison between untreated WT and treated KO mice was included (†). Microscopic analysis: (B) 5× magnification photographs of representative longitudinal spleen sections from each group with hematoxylin-eosin staining, (C-D) and histologic analysis of mouse spleens: (C) concentration of lymphoid nodules per square millimeter, (D) and amount of white pulp (indicator of myeloproliferation). Short-term: 6-month-old mice, after 3 months of diet with or without pacritinib. Long-term: 9-month-old mice, after 6 months of diet with or without pacritinib. Graphs represent percentage of total for each value. #: p≤0.05, **: p≤0.01, ***/###: p≤0.001, ****/####/††††: p≤0.0001 (n=8–10/group).

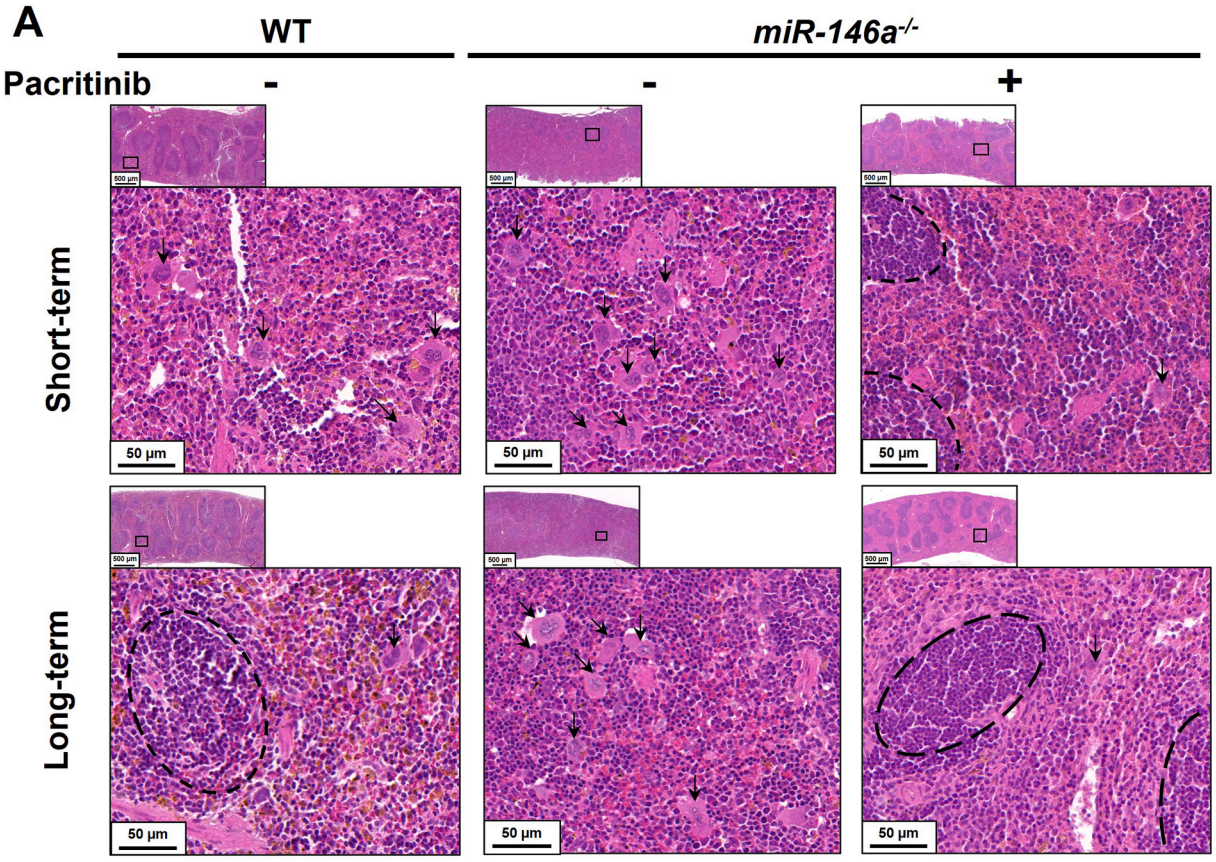

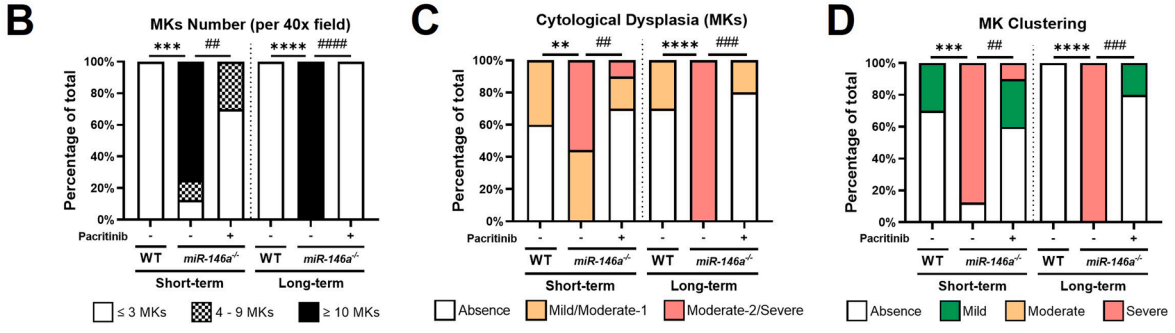

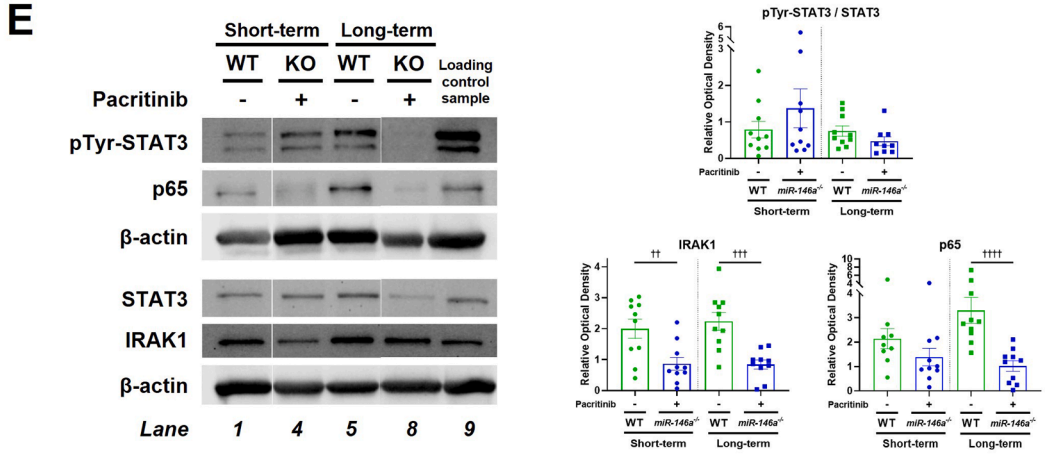

(caption on next page)

Fig. 4. Dual JAK2/IRAK1 inhibition prevented extramedullary hematopoiesis and development of dysplastic megakaryocytes (MKs) in mouse spleen. (A) Photomicrographs of representative longitudinal spleen sections from each group stained with hematoxylin-eosin at 5× and 40× magnification. Dashed lines delineate defined white pulp (lymphoid tissue) and arrows indicate MKs. (B-D) Histological analysis of MKs in mouse spleens: (B) MK count (indicator of extramedullary hematopoiesis), (C) cytological dysplasia of MKs (categorized by the number of dysplastic MKs: absence (0 %), mild/moderate-1 (1–50 %), and moderate-2/severe (>50 %)) (D) and architectural dysplasia of MKs (classification based on the number and size of clusters of MKs). (E) Total cell lysates in spleen of mice, at endpoint. *Left:* Representative western blot image (total spleen lysates from female mice) of 9 experiments. *Right:* Densitometry analysis of western blots of JAK/STAT pathway proteins (pTyr-STAT3/STAT3 ratio, *top*) and NF-κB pathway proteins (IRAK1 and p65, *bottom*) (n=8–10/group). The relative optical density was calculated by normalizing the signal of the protein by that of β-actin and dividing it by the normalized signal of the loading control sample. Outliers were removed using the ROUT method (Q=0.1 %). Graphs represent mean±SEM. Short-term: 6-month-old mice, after 3 months of diet with or without pacritinib. Long-term: 9-month-old mice, after 6 months of diet with or without pacritinib. **/##: p≤0.01, ***/###: p≤0.001, ****/####: p≤0.0001 (n=8–10/group).

anemia in the long-term by blocking ACVR1 [47]. Regarding platelets, pacritinib increased platelet counts from KO groups for both tested treatment-times, with a greater increase after long-term treatment, even exceeding that observed in age-matched WT. Our results are consistent with the increase observed in platelets from thrombocytopenic patients with MF treated with pacritinib [48]. In fact, pacritinib is the only JAK inhibitor approved by the FDA for MF patients with platelet counts below 50,000/μL [48,49]. Although the exact mechanisms are not fully understood, it appears that pacritinib improves hematopoietic function by targeting IRAK1 [43,50]. Indeed, in the same mice model, we have recently shown that both pacritinib and BMS-345541 -a specific NF-κB inhibitor via IKKα/β, downstream of IRAK1- reverse thrombocytopenia, nearly restoring the levels observed in WT mice [43]. This effect was also observed in a study using a SET-2 xenograft model [51], and could be explained by IRAK1 inhibition, as an IRAK1 inhibitor (IRAK1/4 inhibitor, I5409) was able to increase platelet count in a myelodysplastic syndrome xenograft mouse model [50]. Conversely, although an increase in platelet counts has been observed in patients treated with pacritinib, the platelet overshooting that occurs in the long-term treated mice was not observed in MPN patients. This effect may be influenced by other additional factors. For instance, we did observe that long-term pacritinib treatment reduced spleen mass in KO mice, being smaller than age-matched WT mice. This decline could diminish platelet spleen reservoir and therefore increase the number of circulating platelets.

As expected, *miR-146a*$^{-/-}$ mice showed a significant increase in plasma levels of proinflammatory cytokines (IL-1β, CXCL1) compared to WT mice. Concordantly, *Il1b* expression levels were also increased in spleen and bone marrow. Although previous studies suggested that increased IL-1β levels can be specifically induced by *JAK2*V617F [52], our results showed that IL-1β levels were also increased in the *miR-146a*$^{-/-}$ model lacking *JAK2*V617F. In fact, other two murine models of MF-like disease, lacking classical driver mutations, but with inflammatory signaling alteration, via MYC/alarmin axis [16], or IL-1 receptor antagonist (IL-1rn) [17], have been recently described. Notably, pacritinib therapy prevented the increase in CXCL1 and TNF-α levels, after 3 and 6 months of treatment, respectively. In addition to inflammatory responses, CXCL1 has been implicated in tumorigenesis [53–55], and fibrosis [56]. Thus, BM from fibrotic *Gata1*^{low} mice contained higher levels of CXCL1 than BM from WT mice [57]. In humans, CXCL1 may play a similar role to interleukin-8 (IL-8/CXCL8), as both chemokines can signal through the same receptor (CXCR2) [55]. Importantly, CXCR2 signaling mediates BM fibrosis, blockage of the CXCR1/2 axis appears to be able to reduce BM fibrosis and megakaryocyte dysmorphia in murine models [19,58], and high plasma IL-8 levels have a prognostic impact in MF patients [59]. Plasma TNF-α levels are also elevated in patients with PV, ET or MF [10] and are associated with erythropoiesis dysregulation under inflammatory stress [60]. Together, the overall increase in proinflammatory cytokines in the plasma of KO mice is consistent with that found in MF patients [59,61], which may be involved in suppression of T cells [62], immune evasion, and disease progression. The improvement of inflammatory symptoms in MF patients receiving pacritinib, which does not inhibit JAK1, could be explained by IRAK1 inhibition, as shown by JQ1, a BETi that indirectly targets NF-κB [13].

miR-146a$^{-/-}$ mice also developed splenomegaly because of extramedullary hematopoiesis. This is consistent with what occurs in human MF to compensate for inefficient hematopoiesis [20]. The spleen of MF patients contains malignant HSPC [63], and scRNAseq analysis has shown that these reservoirs have unique molecular and functional characteristics that can be therapeutically targeted [64]. Notably, our results showed that none of the pacritinib-treated KO mice developed splenomegaly, and most of them, particularly after long-term treatment, did not exhibit features of myeloproliferation or extramedullary hematopoiesis. Although reduction of splenomegaly has been the main endpoint in clinical trials in patients with myelofibrosis [5], to our knowledge there is no information on the effect of JAK inhibitors on splenic extramedullary hematopoiesis.

Notably, pacritinib-treated *miR-146a*$^{-/-}$ mice did not show reticulin fibrosis, osteosclerosis or increased *Tgfb1* expression levels. This last being one of the main actors for fibrotic process in MPN subjects [65–68]. These results agree with our recent findings, showing that NF-κB inhibition, with both BMS-345541 and pacritinib (targeting IKKα/β or IRAK1, respectively) revert fibrosis and osteosclerosis in old *miR-146a*$^{-/-}$ mice with the established myelofibrotic phenotype [43]. Moreover, in the context of JAK2 mutated clonal hematopoiesis (*e.g.* SET-2 cells), we confirmed that collagen expression was reduced when cells were preincubated with pacritinib before collagen induction with TGF-β. This is particularly relevant because other available JAK inhibitors in monotherapy (such as ruxolitinib and momelotinib) have no clinically significant effect on reducing fibrosis [69,70]. Pacritinib, in contrast, has recently shown a correlation between fibrosis reduction and transfusion independence [71] and between fibrosis reduction and platelet improvement [72] (based on a retrospective review of the PERSIST-2 clinical trial for MF patients) [71,72]. This is a further demonstration that dual JAK2/NF-κB blockade leads to meaningful fibrosis reduction, in line with our previous observations in miR-146a deficient mice [43]. Furthermore, combinations of JAK and BET inhibitors that indirectly target NF-κB, such as pelabresib [73] in combination with ruxolitinib, also showed improvement in BM fibrosis in patients with MF in previous studies [74]. Altogether, our results are consistent with those suggesting that ablation of NF-κB cascade (via IRAK1 or IRAK4), may be more beneficial for MPN patients than exclusively targeting JAK2, with the potential to reduce hematologic toxicities [75].

Clinical phenotype of MF, driver by biological factors, outside of classic driver mutations, also occur in non-clonal diseases (*i.e.* autoimmune diseases), other hemopathies [65,76], or even in triple negative MF [16]. In such cases, drugs or combinations that target the inflammatory component and fibrosis, such as pacritinib, may have therapeutic potential [5,77]. In addition, pacritinib has recently been shown to reverse not only BM fibrosis *in vivo* [43], but also liver fibrosis in mice, positioning it as a potential therapy for patients with liver fibrosis [78].

Other disease-modifying agents are being investigated to prevent progression of MPN to more advanced stages, and targeting inflammation is becoming increasingly important [14,18,19,79]. In fact, inhibition of IL-1β by anti-IL-1β antibodies and the use of reparixin (a CXCR1/2 inhibitor targeting IL-8 signaling) can also reduce BM fibrosis and osteosclerosis in *JAK2*V617F [80] human and *MPL*W515L mice [19], and is the basis for new clinical trials (NCT05835466). Potentially, the use of IL-1RN (IL-1R antagonist) enhancers could also be used as a

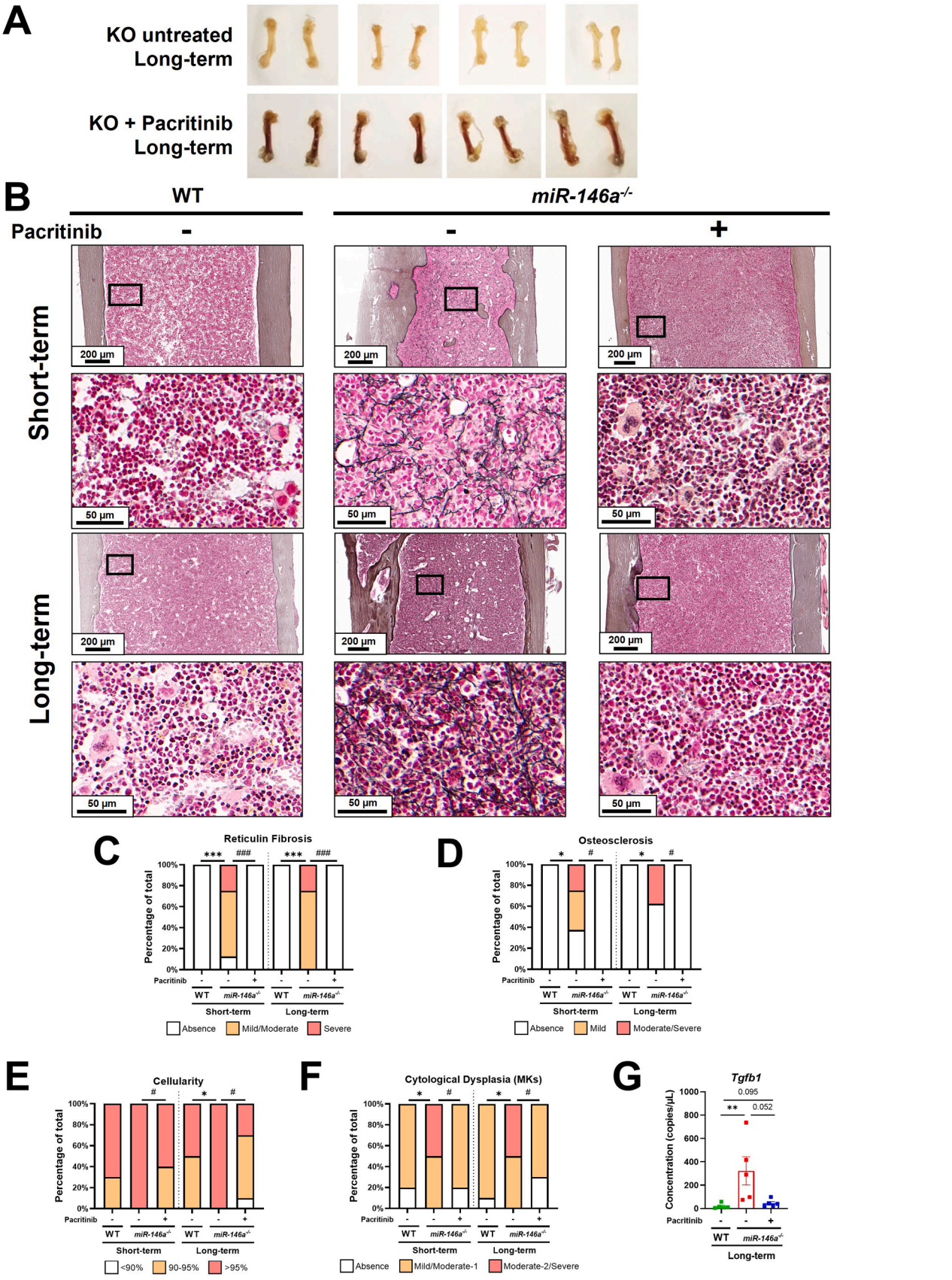

(caption on next page)

Fig. 5. Dual JAK2/IRAK1 inhibition significantly attenuated the myelofibrotic phenotype and osteosclerosis in *miR-146a*$^{-/-}$ (KO) mice. (A) Photographs of representative mouse femurs (9-month-old KO mice, after 6 months of diet) with (*bottom*) or without pacritinib (*top*), in which the natural reddish color of the bone marrow may or may not be observed. (B) 10× and 40× magnification photographs of longitudinal sections of femoral bone marrow with reticulin staining, representative of each group (median of reticulin fibrosis). (C-F) Histological analysis of mouse bone marrow, (C) reticulin fibrosis, (D) osteosclerosis, (E) cellularity, and (F) cytological dysplasia of megakaryocytes, MKs (categorized by the number of dysplastic MKs: absence (0 %), mild/moderate-1 (1–50 %), and moderate-2/severe (>50 %)). (G) Expression levels of *Tgfb1* in bone marrow from C57BL/6 J (WT) and *miR-146a*$^{-/-}$ (KO) at endpoint. Outliers were removed using the ROUT method (Q=0.1 %). Short-term: 6-month-old mice, after 3 months of diet with or without pacritinib. Long-term: 9-month-old mice, after 6 months of diet with or without pacritinib. Graphs represent percentage of total for each value (C-F) or mean±SEM (G). */#: p≤0.05, **: p≤0.01, ***/###: p≤0.001 (n=5–10/group).

protective effect, as IL-1RN deletion in mice induces changes in the BM microenvironment, including fibrosis [17].

5. Conclusion

In conclusion, through this research we found that in an environment of exacerbated chronic inflammation, early intervention with a dual IRAK1/JAK2 inhibitor, such as pacritinib, has a beneficial effect in preventing anemia, thrombocythemia, splenomegaly, and BM fibrosis. Early therapeutic suppression of chronic inflammation, thereby inhibiting the vicious cycle that promotes MPN progression, may be beneficial in MPN patients at high risk for progression to more advanced stages (*e.g.* those with prefibrotic MF).

Ethics approval and consent to participate

This study was approved by the Ethical Committee on Animal Experimentation (CEEA) of the University of Murcia and CARM (reference A13200603).

Funding

This work was supported by CTI BioPharma Corp, a Sobi company (CFE/BI/72–19), and by the Instituto de Salud Carlos III (grants PI18/00316, PI21/00347, PI23/00027). EJC-Z is supported by the Ministry of Science, Innovation and Universities (training of university teachers' program, grant FPU18/03189) and by Spanish Foundation of Hematology and Hemotherapy: Research Grants (Call 2023). MLM is supported by Next Generation EU (grant PMP21/00052).

CRediT authorship contribution statement

Francisca Ferrer-Marín: Writing – review & editing, Supervision, Project administration, Methodology, Funding acquisition, Conceptualization. **Constantino Martínez:** Resources, Methodology, Funding acquisition. **Ernesto José Cuenca-Zamora:** Writing – original draft, Visualization, Methodology, Investigation, Formal analysis. **Pedro Jesús Guijarro-Carrillo:** Methodology, Investigation. **María Luz Morales:** Writing – review & editing, Methodology, Investigation. **Carlos Alcolea-Guardiola:** Investigation, Methodology. **María Luisa Lozano:** Writing – review & editing. **María José López-Poveda:** Writing – review & editing, Validation, Methodology, Investigation, Formal analysis. **Raúl Teruel-Montoya:** Writing – review & editing, Visualization, Supervision, Project administration, Methodology, Formal analysis, Conceptualization. **Rocío Gonzalez-Conejero:** Writing – review & editing, Methodology, Funding acquisition. **Natalia Vidal-Garrido:** Investigation, Methodology.

Declaration of Competing Interest

The authors declare the following financial interests/personal relationships which may be considered as potential competing interests. Francisca Ferrer-Marin reports a relationship with CTI BioPharma Corp, a Sobi company, that includes: funding grants (CFE/BI/72–19). If there are other authors, they declare that they have no known competing financial interests or personal relationships that could have appeared to influence the work reported in this paper

Acknowledgments

The authors thank Nuria Garcia-Barbera for her assistance in the animal facility. We also thank Paula Durán-Espín for her technical assistance in the laboratory.

Supplementary information

Supplementary Material. This file includes all the supplementary material, figures, tables and legends that are mentioned in the main text.

Appendix A. Supporting information

Supplementary data associated with this article can be found in the online version at doi:10.1016/j.biopha.2024.117712.

Data availability

All data from this study will be freely accessible upon request to the corresponding authors.

References

1 D.A. Arber, A. Orazi, R.P. Hasserjian, M.J. Borowitz, K.R. Calvo, H.-M. Kvasnicka, et al., International Consensus Classification of Myeloid Neoplasms and Acute Leukemias: integrating morphologic, clinical, and genomic data, Blood 140 (11) (2022) 1200–1228.
2 J.D. Khoury, E. Solary, O. Abla, Y. Akkari, R. Alaggio, J.F. Apperley, et al., The 5th edition of the World Health Organization Classification of Haematolymphoid Tumours: Myeloid and Histiocytic/Dendritic Neoplasms, Leukemia 36 (7) (2022) 1703–1719.
3 S. Cerquozzi, A. Tefferi, Blast transformation and fibrotic progression in polycythemia vera and essential thrombocythemia: a literature review of incidence and risk factors, Blood Cancer J. 5 (11) (2015) e366–e366.
4 N. Szuber, M. Mudireddy, M. Nicolosi, D. Penna, R.R. Vallapureddy, T.L. Lasho, et al., 3023 Mayo Clinic patients with myeloproliferative neoplasms: risk-stratified comparison of survival and outcomes data among disease subgroups, Mayo Clin. Proc. 94 (4) (2019) 599–610.
5 A. Tefferi, Primary myelofibrosis: 2023 update on diagnosis, risk-stratification, and management, Am. J. Hematol. 98 (5) (2023) 801–821.
6 L.E. Aguirre, A. Jain, S. Ball, N. Ali, Al, V.O. Volpe, S. Tinsley-Vance, et al., Triple-Negative Myelofibrosis: Disease Features, Response to Treatment and Outcomes, Clin. Lymphoma Myeloma Leuk. 24 (7) (2024) 459–467.
7 P. Guglielmelli, A. Pacilli, G. Rotunno, E. Rumi, V. Rosti, F. Delaini, et al., Presentation and outcome of patients with 2016 WHO diagnosis of prefibrotic and overt primary myelofibrosis, Blood 129 (24) (2017) 3227–3236.
8 D. Luque Paz, R. Kralovics, R.C. Skoda, Genetic basis and molecular profiling in myeloproliferative neoplasms, Blood 141 (16) (2023) 1909–1921.
9 J. How, J.S. Garcia, A. Mullally, Biology and therapeutic targeting of molecular mechanisms in MPNs, Blood 141 (16) (2023) 1922–1933.
10 S. Koschmieder, T.I. Mughal, H.C. Hasselbalch, G. Barosi, P. Valent, J.-J. Kiladjian, et al., Myeloproliferative neoplasms and inflammation: whether to target the malignant clone or the inflammatory process or both, Leukemia 30 (5) (2016) 1018–1024.
11 S. Rai, Y. Zhang, E. Grockowiak, Q. Kimmerlin, N. Hansen, C.B. Stoll, et al., IL-1β promotes MPN disease initiation by favoring early clonal expansion of JAK2-mutant hematopoietic stem cells, Blood Adv. 8 (5) (2024) 1234–1249.
12 M. Kleppe, M. Kwak, P. Koppikar, M. Riester, M. Keller, L. Bastian, et al., JAK-STAT pathway activation in malignant and nonmalignant cells contributes to MPN pathogenesis and therapeutic response, Cancer Discov. 5 (3) (2015) 316–331.
13 M. Kleppe, R. Koche, L. Zou, P. van Galen, C.E. Hill, L. Dong, et al., Dual Targeting of Oncogenic Activation and Inflammatory Signaling Increases Therapeutic Efficacy in Myeloproliferative Neoplasms, Cancer Cell 33 (1) (2018) 29–43.e7.
14 M.F.-U. Rahman, Y. Yang, B.T. Le, A. Dutta, J. Posyniak, P. Faughnan, et al., Interleukin-1 contributes to clonal expansion and progression of bone marrow fibrosis in JAK2V617F-induced myeloproliferative neoplasm, Nat. Commun. 13 (1) (2022) 5347.

15 H.F.E. Gleitz, A.J.F. Dugourd, N.B. Leimkühler, I.A.M. Snoeren, S.N.R. Fuchs, S. Menzel, et al., Increased CXCL4 expression in hematopoietic cells links inflammation and progression of bone marrow fibrosis in MPN, Blood 136 (18) (2020) 2051–2064.
16 N.D. Vincelette, X. Yu, A.T. Kuykendall, J. Moon, S. Su, C.-H. Cheng, et al., Trisomy 8 Defines a Distinct Subtype of Myeloproliferative Neoplasms Driven by the MYC–Alarmin Axis, Blood Cancer Discov. 5 (4) (2024) 276–297.
17 A. Villatoro, V. Cuminetti, A. Bernal, C. Torroja, I. Cossío, A. Benguría, et al., Endogenous IL-1 receptor antagonist restricts healthy and malignant myeloproliferation, Nat. Commun. 14 (1) (2023) 12.
18 J. Mascarenhas, H.F.E. Gleitz, H.T. Chifotides, C.N. Harrison, S. Verstovsek, A. M. Vannucchi, et al., Biological drivers of clinical phenotype in myelofibrosis, Leukemia 37 (2) (2023) 255–264.
19 A. Dunbar, D. Kim, M. Lu, M. Farina, R.L. Bowman, J.L. Yang, et al., CXCL8/CXCR2 signaling mediates bone marrow fibrosis and represents a therapeutic target in myelofibrosis, Blood 141 (20) (2023) 2508–2519.
20 D. Cenariu, S. Iluta, A.-A. Zimta, B. Petrushev, L. Qian, N. Dirzu, et al., Extramedullary Hematopoiesis of the Liver and Spleen, J. Clin. Med 10 (24) (2021) 5831.
21 K. Taniguchi, M. Karin, NF-κB, inflammation, immunity and cancer: coming of age, Nat. Rev. Immunol. 18 (5) (2018) 309–324.
22 A. Salas, C. Hernandez-Rocha, M. Duijvestein, W. Faubion, D. McGovern, S. Vermeire, et al., JAK–STAT pathway targeting for the treatment of inflammatory bowel disease, Nat. Rev. Gastroenterol. Hepatol. 17 (6) (2020) 323–337.
23 G. Liu, Y.-J. Park, E. Abraham, Interleukin-1 receptor-associated kinase (IRAK) -1-mediated NF-kappaB activation requires cytosolic and nuclear activity, FASEB J. 22 (7) (2008) 2285–2296.
24 S.I. Grivennikov, M. Karin, Dangerous liaisons: STAT3 and NF-κB collaboration and crosstalk in cancer, Cytokine Growth Factor Rev. 21 (1) (2010) 11–19.
25 J.W. Singer, A. Fleischman, S. Al-Fayoumi, J.O. Mascarenhas, Q. Yu, A. Agarwal, Inhibition of interleukin-1 receptor-associated kinase 1 (IRAK1) as a therapeutic strategy, Oncotarget 9 (70) (2018) 33416–33439.
26 D.A.C. Fisher, O. Malkova, E.K. Engle, C.A. Miner, M.C. Fulbright, G.K. Behbehani, et al., Mass cytometry analysis reveals hyperactive NF Kappa B signaling in myelofibrosis and secondary acute myeloid leukemia, Leukemia 31 (9) (2017) 1962–1974.
27 D.E. Rothschild, D.K. McDaniel, V.M. Ringel-Scaia, I.C. Allen, Modulating inflammation through the negative regulation of NF-κB signaling, J. Leukoc. Biol. 103 (6) (2018) 1131–1150.
28 J.L. Zhao, D.S. Rao, M.P. Boldin, K.D. Taganov, R.M. O'Connell, D. Baltimore, NF-κB dysregulation in microRNA-146a–deficient mice drives the development of myeloid malignancies, Proc. Natl. Acad. Sci. 108 (22) (2011) 9184–9189.
29 M.P. Boldin, K.D. Taganov, D.S. Rao, L. Yang, J.L. Zhao, M. Kalwani, et al., miR-146a is a significant brake on autoimmunity, myeloproliferation, and cancer in mice, J. Exp. Med. 208 (6) (2011) 1189–1201.
30 N. Magilnick, E.Y. Reyes, W.-L. Wang, S.L. Vonderfecht, J. Gohda, J. Inoue, et al., miR-146a – Traf6 regulatory axis controls autoimmunity and myelopoiesis, but is dispensable for hematopoietic stem cell homeostasis and tumor suppression, Proc. Natl. Acad. Sci. 114 (34) (2017) E7140–E7149.
31 F. Ferrer-Marín, A.B. Arroyo, B. Bellosillo, E.J. Cuenca, L. Zamora, J.M. Hernández-Rivas, et al., miR-146a rs2431697 identifies myeloproliferative neoplasm patients with higher secondary myelofibrosis progression risk, Leukemia 34 (10) (2020) 2648–2659.
32 S. Jacquelin, F. Kramer, A. Mullally, S.W. Lane, Murine models of myelofibrosis, Cancers (Basel) 12 (9) (2020) 2381.
33 L. Belver, A.A. Ferrando, Aberrant cytokine production by nonmalignant cells in the pathogenesis of myeloproliferative tumors and response to JAK inhibitor therapies, Cancer Discov. 5 (3) (2015) 234–236.
34 S. Aref, D. Atia, Tantawy A. Al, M. Al Boghdady, E. Gouda, Predictive Value of miR-146a rs2431697 Polymorphism to Myelofibrosis Progression in Patients with Myeloproliferative Neoplasm, Asian Pac. J. Cancer Prev. 22 (11) (2021) 3585–3589.
35 H.F.E. Gleitz, A. Benabid, R.K. Schneider, Still a burning question: the interplay between inflammation and fibrosis in myeloproliferative neoplasms, Curr. Opin. Hematol. 28 (5) (2021) 364–371.
36 S. Verstovsek, R. Mesa, M. Talpaz, J.J. Kiladjian, C.N. Harrison, S.T. Oh, et al., Retrospective analysis of pacritinib in patients with myelofibrosis and severe thrombocytopenia, Haematologica 107 (7) (2022) 1599–1607.
37 J. Mascarenhas, Pacritinib for the treatment of patients with myelofibrosis and thrombocytopenia, Expert Rev. Hematol. 15 (8) (2022) 671–684.
38 J. Thiele, R. Fischer, Megakaryocytopoiesis in haematological disorders: Diagnostic features of bone marrow biopsies, Virchows Arch. A Pathol. Anat. Histopathol. 418 (2) (1991) 87–97.
39 D.P. O'Malley, Y.S. Kim, S.L. Perkins, L. Baldridge, B.E. Juliar, A. Orazi, Morphologic and immunohistochemical evaluation of splenic hematopoietic proliferations in neoplastic and benign disorders, Mod. Pathol. 18 (12) (2005) 1550–1561.
40 M. Moonim, A. Porwit, Normal bone marrow histology. Blood and Bone Marrow Pathology, Elsevier, 2011, pp. 45–62.
41 J. Thiele, H.M. Kvasnicka, F. Facchetti, V. Franco, J. van der Walt, A. Orazi, European consensus on grading bone marrow fibrosis and assessment of cellularity, Haematologica 90 (8) (2005) 1128–1132.
42 H.M. Kvasnicka, C. Beham-Schmid, R. Bob, S. Dirnhofer, K. Hussein, H. Kreipe, et al., Problems and pitfalls in grading of bone marrow fibrosis, collagen deposition and osteosclerosis – a consensus-based study, Histopathology 68 (6) (2016) 905–915.
43 E.J. Cuenca-Zamora, P.J. Guijarro-Carrillo, M.J. López-Poveda, M.L. Morales, M. L. Lozano, R. Gonzalez-Conejero, et al., *miR-146a* $^{-/-}$ mice model reveals that NF-κB inhibition reverts inflammation-driven myelofibrosis-like phenotype, Am. J. Hematol. 99 (7) (2024) 1326–1337.
44 M. Mann, A. Mehta, J.L. Zhao, K. Lee, G.K. Marinov, Y. Garcia-Flores, et al., An NF-κB-microRNA regulatory network tunes macrophage inflammatory responses, Nat. Commun. 8 (1) (2017) 851.
45 S. Verstovsek, J. Kiladjian, A.M. Vannucchi, R.A. Mesa, P. Squier, J.E. Hamer-Maansson, et al., Early intervention in myelofibrosis and impact on outcomes: A pooled analysis of the COMFORT-I and COMFORT-II studies, Cancer 129 (11) (2023) 1681–1690.
46 R.A. Mesa, A.M. Vannucchi, A. Mead, M. Egyed, A. Szoke, A. Suvorov, et al., Pacritinib versus best available therapy for the treatment of myelofibrosis irrespective of baseline cytopenias (PERSIST-1): an international, randomised, phase 3 trial, Lancet Haematol. 4 (5) (2017) e225–e236.
47 S.T. Oh, R.A. Mesa, C.N. Harrison, P. Bose, A.T. Gerds, V. Gupta, et al., Pacritinib is a potent ACVR1 inhibitor with significant anemia benefit in patients with myelofibrosis, Blood Adv. 7 (19) (2023) 5835–5842.
48 J. Mascarenhas, R. Hoffman, M. Talpaz, A.T. Gerds, B. Stein, V. Gupta, et al., Pacritinib vs Best Available Therapy, Including Ruxolitinib, in Patients With Myelofibrosis: A Randomized Clinical Trial, JAMA Oncol. 4 (5) (2018) 652–659.
49 Y.N. Lamb, Pacritinib: First Approval, Drugs 82 (7) (2022) 831–838.
50 G.W. Rhyasen, L. Bolanos, J. Fang, A. Jerez, M. Wunderlich, C. Rigolino, et al., Targeting IRAK1 as a therapeutic approach for myelodysplastic syndrome, Cancer Cell 24 (1) (2013) 90–104.
51 S. Hart, K.C. Goh, V. Novotny-Diermayr, C.Y. Hu, H. Hentze, Y.C. Tan, et al., SB1518, a novel macrocyclic pyrimidine-based JAK2 inhibitor for the treatment of myeloid and lymphoid malignancies, Leukemia 25 (11) (2011) 1751–1759.
52 S. Allain-Maillet, A. Bosseboeuf, N. Mennesson, M. Bostoën, L. Dufeu, E.H. Choi, et al., Anti-Glucosylsphingosine Autoimmunity, JAK2V617F-Dependent Interleukin-1β and JAK2V617F-Independent Cytokines in Myeloproliferative Neoplasms, Cancers (Basel) 12 (9) (2020).
53 P. Dhawan, A. Richmond, Role of CXCL1 in tumorigenesis of melanoma, J. Leukoc. Biol. 72 (1) (2002) 9–18.
54 Y.-L. Hsu, Y.-J. Chen, W.-A. Chang, S.-F. Jian, H.-L. Fan, J.-Y. Wang, et al., Interaction between Tumor-Associated Dendritic Cells and Colon Cancer Cells Contributes to Tumor Progression via CXCL1, Int J. Mol. Sci. 19 (8) (2018) 2427.
55 X. Chen, R. Jin, R. Chen, Z. Huang, Complementary action of CXCL1 and CXCL8 in pathogenesis of gastric carcinoma, Int J. Clin. Exp. Pathol. 11 (2) (2018) 1036–1045.
56 C.-L. Wu, R. Yin, S.-N. Wang, R. Ying, A Review of CXCL1 in Cardiac Fibrosis, Front Cardiovasc Med 8 (2021) 674498.
57 M. Zingariello, P. Verachi, F. Gobbo, F. Martelli, M. Falchi, M. Mazzarini, et al., Resident self-tissue of proinflammatory cytokines rather than their systemic levels correlates with development of myelofibrosis in Gata1low mice, Biomolecules 12 (2) (2022) 234.
58 G. Vermeersch, P. Proost, S. Struyf, M. Gouwy, T. Devos, CXCL8 and its cognate receptors CXCR1/CXCR2 in primary myelofibrosis, Haematologica 109 (2) (2024) 2060–2072.
59 A. Tefferi, R. Vaidya, D. Caramazza, C. Finke, T. Lasho, A. Pardanani, Circulating interleukin (IL)-8, IL-2R, IL-12, and IL-15 levels are independently prognostic in primary myelofibrosis: a comprehensive cytokine profiling study, J. Clin. Oncol. 29 (10) (2011) 1356–1363.
60 A. Guerra, V. Lo Presti, A.C. Martins, C. Castruccio Castracani, R. Gupta, R. Oikonomidou, et al., TNFα Controls the Delicate Balance between Erythropoiesis and Stem Cell Exhaustion during Inflammatory Stress, Blood 138 (ement 1) (2021), 2184–2184.
61 D.A.C. Fisher, C.A. Miner, E.K. Engle, H. Hu, T.B. Collins, A. Zhou, et al., Cytokine production in myelofibrosis exhibits differential responsiveness to JAK-STAT, MAP kinase, and NFκB signaling, Leukemia 33 (8) (2019) 1978–1995.
62 M.E. Groh, B. Maitra, E. Szekely, O.N. Koç, Human mesenchymal stem cells require monocyte-mediated activation to suppress alloreactive T cells, Exp. Hematol. 33 (8) (2005) 928–934.
63 X. Wang, S. Prakash, M. Lu, J. Tripodi, F. Ye, V. Najfeld, et al., Spleens of myelofibrosis patients contain malignant hematopoietic stem cells, J. Clin. Invest 122 (11) (2012) 3888–3899.
64 N. Mende, H.P. Bastos, A. Santoro, K.T. Mahbubani, V. Ciaurro, E.F. Calderbank, et al., Unique molecular and functional features of extramedullary hematopoietic stem and progenitor cell reservoirs in humans, Blood 139 (23) (2022) 3387–3401.
65 K. Ghosh, D.K. Shome, B. Kulkarni, M.K. Ghosh, K. Ghosh, Fibrosis and bone marrow: understanding causation and pathobiology, J. Transl. Med 21 (1) (2023) 703.
66 W. Vainchenker, N. Yahmi, V. Havelange, C. Marty, I. Plo, S.N. Constantinescu, Recent advances in therapies for primary myelofibrosis, Fac. Rev. 12 (2023).
67 J.-C. Yao, K.A. Oetjen, T. Wang, H. Xu, G. Abou-Ezzi, J.R. Krambs, et al., TGF-β signaling in myeloproliferative neoplasms contributes to myelofibrosis without disrupting the hematopoietic niche, J. Clin. Investig. 132 (11) (2022).
68 C. Aoun, N. Maslah, S. Ganesan, N. Salomao, R. Gendron, S. Awan Toor, et al., <scp>JAK2V617F</scp> -dependent down regulation of <scp>SHP</scp> -1 expression participates in the selection of myeloproliferative neoplasm cells in the presence of <scp>TGF</scp> -β, J. Cell Mol. Med 28 (20) (2024) e70138.
69 J. Mascarenhas, R. Hoffman, Ruxolitinib: The First FDA Approved Therapy for the Treatment of Myelofibrosis, Clin. Cancer Res. 18 (11) (2012) 3008–3014.
70 S.T. Oh, S. Verstovsek, V. Gupta, U. Platzbecker, T. Devos, J.-J. Kiladjian, et al., Changes in bone marrow fibrosis during momelotinib or ruxolitinib therapy do not correlate with efficacy outcomes in patients with myelofibrosis, EJHaem 5 (1) (2024) 105–116.
71 S.T. Oh, J. Shammo, V. Gupta, M.F. McMullin, P. Bose, R.A. Mesa, et al., Retrospective Analysis of the Relationship between Transfusion Independence and

Bone Marrow Fibrosis Reduction in Patients with Myelofibrosis Treated with Pacritinib Versus Ruxolitinib, Blood 142 (ement 1) (2023), 4566–4566.
72 P. Vachhani, A. Yacoub, E. Traer, L. Benajiba, F. Passamonti, A. Kishtagari, et al., Platelet Response in Pacritinib-Treated Patients with Cytopenic Myelofibrosis: A Retrospective Analysis of PERSIST-2 and PAC203 Studies, Blood 142 (ement 1) (2023), 4554–4554.
73 R.K. Rampal, S. Grosicki, D. Chraniuk, E. Abruzzese, P. Bose, A.T. Gerds, et al., Pelabresib in Combination with Ruxolitinib for Janus Kinase Inhibitor Treatment-Naïve Patients with Myelofibrosis: Results of the MANIFEST-2 Randomized, Double-Blind, Phase 3 Study, Blood 142 (ement 1) (2023), 628–628.
74 J. Mascarenhas, M. Kremyanskaya, A. Patriarca, F. Palandri, T. Devos, F. Passamonti, et al., MANIFEST: Pelabresib in Combination With Ruxolitinib for Janus Kinase Inhibitor Treatment-Naïve Myelofibrosis, J. Clin. Oncol. 41 (32) (2023) 4993–5004.
75 A.B.A. Laranjeira, T. Kong, S.C. Snyder, M.C. Fulbright, D.A.C. Fisher, D. T. Starczynowski, et al., In vivo ablation of NFκB cascade effectors alleviates disease burden in myeloproliferative neoplasms, Blood (2024).
76 Y. Tanaka, Y. Luo, J.J. O'Shea, S. Nakayamada, Janus kinase-targeting therapies in rheumatology: a mechanisms-based approach, Nat. Rev. Rheuma 18 (3) (2022) 133–145.
77 D. Tremblay, R. Mesa, Novel treatments for myelofibrosis: beyond JAK inhibitors, Int J. Hematol. 115 (5) (2022) 645–658.
78 S. Torres, C. Ortiz, N. Bachtler, W. Gu, L.D. Grünewald, N. Kraus, et al., Janus kinase 2 inhibition by pacritinib as potential therapeutic target for liver fibrosis, Hepatology 77 (4) (2023) 1228–1240.
79 J.C. Balandrán, A. Lasry, I. Aifantis, The role of inflammation in the initiation and progression of myeloid neoplasms, Blood Cancer Discov. 4 (4) (2023) 254–266.
80 S. Rai, E. Grockowiak, N. Hansen, D. Luque Paz, C.B. Stoll, H. Hao-Shen, et al., Inhibition of interleukin-1β reduces myelofibrosis and osteosclerosis in mice with JAK2-V617F driven myeloproliferative neoplasm, Nat. Commun. 13 (1) (2022) 5346.